DOI: 10.1007/s10967-007-6877-9 *Journal of Radioanalytical and Nuclear Chemistry, Vol. 273, No.2 (2007) 443–450*

Efficiency calibration of an HPGe detector in the 0.1–2.5 MeV energy range for Am–Be neutron source-based PGAA applications

Ş. Turhan*

Sarayköy Nuclear Research and Training Center (SNRTC), 06983 Sarayköy, Ankara, Turkey

(Received August 28, 2006)

A 740 GBq ^{241}Am–Be neutron source based prompt gamma-ray activation analysis (PGAA) setup in combination with a typical coaxial n-type HPGe detector (REGe) system was used to analyze light elements like H, B, C, N, etc. The absolute full energy peak (FEP) efficiencies of the shielded REGe detector for irradiation and counting geometries and for sources with different sizes (point, ampoule and cylindrical) were measured in the 0.1–2.5 MeV energy range by utilizing calibrated sources (point, liquid and solid). 4th order polynomials were fitted to the experimental data. Efficiencies in far irradiation and counting geometries are compared.

Introduction

The neutron induced prompt gamma-ray activation analysis (PGAA) is a rapid, non-destructive and commonly used nuclear analytic technique for multi-elemental analysis. This technique is particularly suitable for analyzing of H, B, C, N, S, P, Si and Cd elements, whose determination are difficult by conventional neutron activation analysis (INAA).[1–8] PGAA is based on the detection of capture gamma-rays emitted by a target material (solid, liquid or gaseous) while irradiated with neutrons. In PGAA, the qualitative and quantitative analysis is performed by identifying peaks of characteristic gamma-rays and their net areas.

A prompt gamma-ray spectrometric system, containing REGe, is the heart of the PGAA facility. The absolute full energy peak (FEP) efficiency is one of the most important characteristics of these detectors for a wide energy range, i.e., from 0.1 to 10 MeV and its accurate knowledge is required in almost all works based on absolute methods, such as the precise measurement of gamma-ray emission probabilities, differential and integral cross sections, as well as reaction rate measurements, or the determination of k_0-factors.[9–11] In PGAA applications, efficiency measurements are generally carried out by using calibrated radioactive sources with precisely known half-lives, gamma-ray energies and emission probabilities combined with (n,γ) reactions, such as ^{14}N(n,γ), ^{35}Cl(n,γ), ^{59}Co(n,γ), etc.[12–14]

In the present work, commercially available standard sources, such as a mixed-radionuclide calibration ampoule, a ^{152}Eu single radionuclide source (point and ampoule) and BL3 uranium standard were used to determine the efficiency curve in the energy range of 0.1–2.5 MeV. This energy range is enough for analyzing elements such as ^{1}H (E_γ = 2.22 MeV), ^{10}B (E_γ = 0.48 MeV), ^{14}N (E_γ = 1.89 MeV), ^{16}O (E_γ = 0.87 MeV and 2.18 MeV), ^{19}F (E_γ = 0.58 MeV and 1.63 MeV), ^{31}P (E_γ = 0.64 MeV), ^{35}Cl (E_γ = 0.52 MeV, 0.79 MeV, 1.16 MeV, 1.95 MeV and 1.959 MeV).[6] Under different conditions, i.e., for far irradiation and counting geometries, for sources with different sizes (point, ampoule and cylindrical) the measured FEP efficiencies are fitted with a suitable function to enable the interpolation to other energies of interest.

Experimental

Detection system

The PGAA setup with a 740 GBq ^{241}Am–Be neutron source was installed as shown in Fig. 1. The physical dimensions of the irradiation unit are 132 cm (W) × 132 cm (L) × 103 cm (H). In the present irradiation unit, the neutron source placed in a polypropylene tube was positioned in a 55-cm-diameter cylinder tank made of polypropylene as well. It was coaxially positioned in the geometrical center of lead rings with the thickness of 6 cm (internal diameter: 9 cm, outer diameter: 21 cm and total height: 33 cm). Thus, the gamma-rays emitted directly from the source itself, were reduced substantially by using the lead rings placed in the cylinder tank. The moderator tank was additionally shielded with paraffin in all sides to prevent the detector sides from fast neutrons. The thickness of paraffin at the front side of the tank is 28 cm and other sides of it are 18 cm, respectively. Two surfaces of the neutron irradiation unit was also shielded by using lead bricks in total thickness of 18 cm, and the other surfaces are concrete walls in the thickness of 1 to 2 m in a basement.

* E-mail: seref.turhan@taek.gov.tr

0236–5731/USD 20.00

Akadémiai Kiadó, Budapest
Springer, Dordrecht

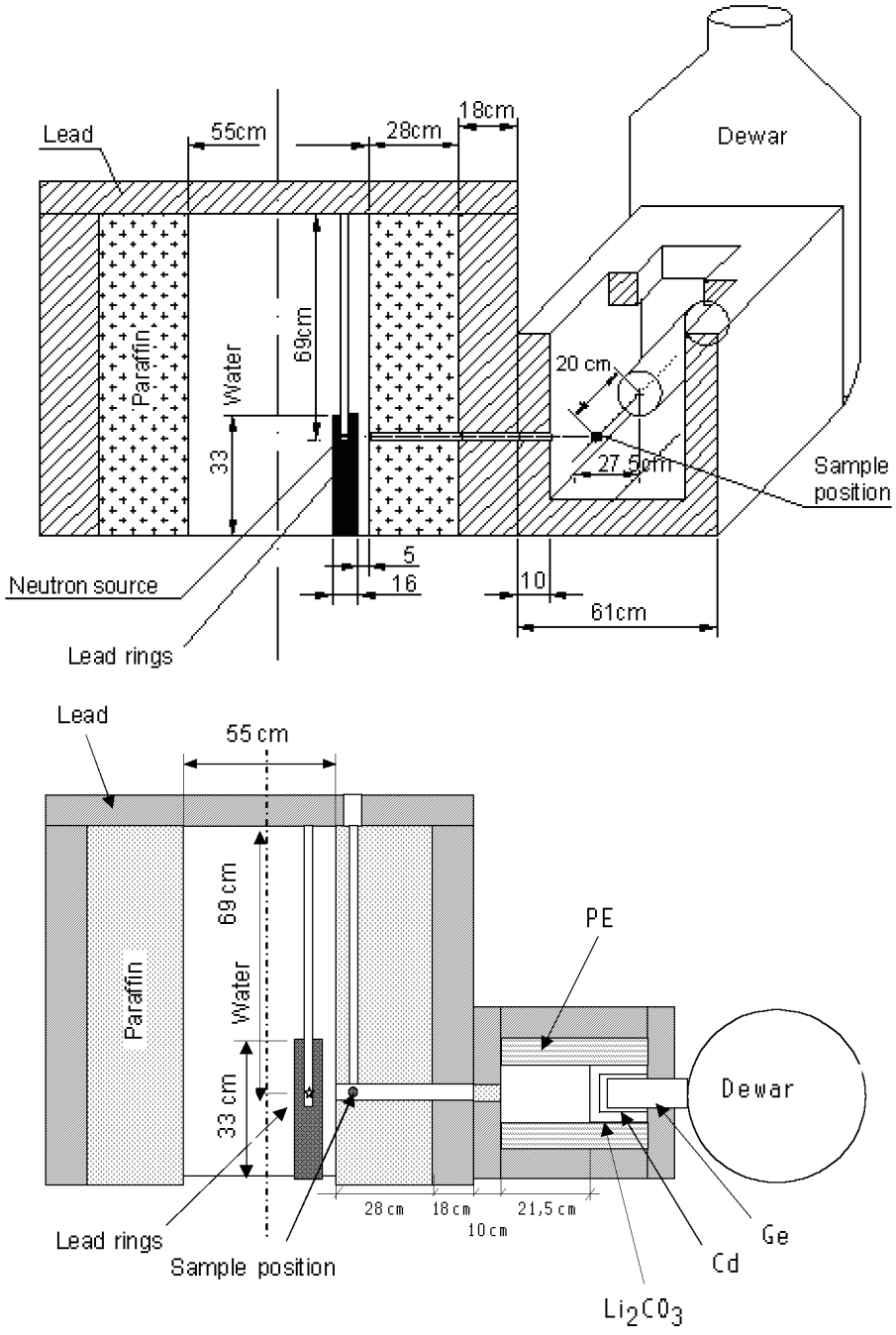

Fig. 1. Schematic layout of the PGAA setup; (a) far irradiation geometry, (b) far counting geometry

The gamma-ray detection system is composed of a REGe detector with its own preamplifier with a side-looking type LN_2 Dewar, a spectroscopy amplifier, an 8K ADC and a conventional Canberra 35^+ type multichannel analyzer (MCA). The REGe detector has a relative efficiency of 22.6%, and energy resolutions of 1.80 keV at 1332.5 keV (^{60}Co) and 0.97 keV at 122 keV (^{57}Co), and a peak-to-Compton ratio of 53.5:1. The present data acquisition system allows the collection of only one type of the spectrum at a time, because a single-input MCA is used.

The REGe detector is also irradiated by neutrons during prompt gamma-ray analysis and it can result in various degrees of damage during a prolonged exposure.[15] Therefore, the detector is shielded with both natural lithium carbonate (Li_2CO_3) powder in a hollow wooden box (powder thickness: 5 cm at front of detector window, 1.5 cm on the sides of the Al end-cap of the

detector) and also 1 mm thick cadmium cover against thermal neutrons. The ^{6}Li nuclide (7.52% abundance in natural lithium) captures thermal neutrons by the reaction ^{6}Li(n,^{3}H)^{4}He and produces no gamma-rays. Cadmium is an efficient and economical absorber but for thermal neutrons only based on the reaction ^{113}Cd(n,γ)^{114}Cd, producing additional prompt-gammas such as 0.559 MeV and 0.651 MeV, etc. Polyethylene bricks with the thickness of 5 cm surround both neutron shields to thermalize any scattered neutrons. This neutron shielding is removable, e.g., during Cd analysis the cylindrical Cd cover is removed from the end-cap of REGe detector. However, the lithium carbonate shielding is removed only when boron is being analyzed. Finally, the detector assembly is surrounded by 10 cm thick lead bricks to reduce gamma-ray background.

Counting geometry

The sample irradiation layout was designed in two different configurations: first, sample-to-source distance was 96.5 cm, and the REGe detector was located at a distance of about 20 cm from sample position and at an angle of 90° with respect to the neutron beam direction (far irradiation geometry) (Fig. 1a). In the second configuration the sample was kept at the distance of 12.5 cm from the neutron source and the REGe detector was located at a distance of about 77.5 cm from the sample position (far counting geometry) (Fig. 1b).

Efficiency calibration

The absolute FEP efficiency for gamma-rays is energy dependent and sensitive to the source-to-detector geometry. In the ideal case, it can be calculated as the ratio of the number of detected photons of a particular energy to the total number, emitted by the source at that energy:

$$\varepsilon(E_\gamma) = \frac{C}{P_\gamma \cdot A} \qquad (1)$$

where C is the net count rate under the full-energy peak corresponding to E_γ energy photon emitted by a radionuclide with a known activity, A (in Bq), and absolute emission probability P_γ.

In the present work, the FEP efficiencies of the REGe detector for different source–detector configurations (far irradiation and counting geometries) and source sizes (point, ampoule and cylindrical) were measured in the energy range of 0.1–2.5 MeV by using commercially available standard ^{152}Eu point source (supplied by Amersham), mixed-radionuclide solution source (supplied by Isotope Products, 5 ml flame-sealed ampoule, source No: 758-19), which contained ^{109}Cd, ^{57}Co, ^{123m}Te, ^{113}Sn, ^{137}Cs, ^{60}Co and ^{88}Y, and multienergy gamma-ray emitters: ^{152}Eu in the form of a solution (supplied by National Institute and Standards and Technology, SRM 4370C, in a 5-ml flame-sealed ampoule) and BL-3 solid natural uranium standard (Canadian certified reference material, cylindrical shaped with the diameter of 4 cm and height of 6 cm). Background intensities obtained in earlier measurements were subtracted in order to get net counts in the energy regions of interest for BL-3 uranium standard. Even though data are obtained below 100 keV, special problems are connected with the detection of low-energy γ-rays; attenuation being one of them. Therefore, attention will be focused on the 0.1–2.5 MeV regions. The necessary nuclear data of the radionuclides used in efficiency calibration is given in Table 1.

The calibration sources were counted by placing them in the sample position shown in Fig. 1. For the far irradiation geometry the 20 cm sample-to-detector distance reduces the contribution of the random and sum coincidences to a negligible level. Therefore, no coincidence correction was necessary. For the far counting geometry, the 77.5 cm sample-to-detector distance also eliminates the coincidence summing losses.

Various fitting functions suggested for the efficiencies in the literature[12,16–21] were assessed and the experimental data, which were obtained for each configuration and geometry, were fitted to the suitable functions. The fourth order polynomial of the forms:

$$\varepsilon(E_\gamma) = \exp\left(\sum_{i=0}^{4} a_i \left(\ln E_\gamma\right)^i\right) \qquad (2)$$

has been used as fitting functions for the FEP efficiencies of corresponding gamma-ray energies where a_i-s are fitted parameters.

Results

The FEP efficiency values measured in the far irradiation geometry with their associated uncertainties ranging from 1% to 3%, are shown, as functions of the gamma-ray energy, for the point source (i.e., ^{152}Eu, in the range of 0.1–1.5 MeV), for the ampoule (i.e., the mixed source in the range of 0.1–2.0 MeV) and for the cylindrical plastic container (i.e., the BL3 uranium standard in the range of 0.2–2.5 MeV) in Fig. 2a, 2b and 2c, respectively. The FEP efficiency values are in the order of 10^{-3} to 10^{-4}. For the far counting geometry the FEP efficiency values with their associated uncertainties ranging from 1% to 3%, are shown, as functions of the gamma-ray energy as above in Fig. 3a, 3b and 3c, respectively. The FEP efficiency values are in the order of 10^{-5} to 10^{-6}. Because the efficiency curve (Fig. 3a)

obtained for point source differs from the other curves the measured data were fitted to the following function instead of the function given in Eq. (2):

$$\varepsilon(E_\gamma) = \exp\left(\frac{1}{E_\gamma} \cdot \sum_{i=1}^{4} a_i \left(\ln E_\gamma \right)^{i-1} \right) \qquad (3)$$

where a_i-s are fitted parameters.

The ratios of the fitted efficiency data of the voluminous sources to the point source efficiency in the range of 0.1–1.5 MeV for far irradiation and counting geometries are calculated and given in Fig 4a and 4b, respectively.

Table 1. Nuclear data of calibration sources used for the determination of efficiency calibration

Calibration source	Activity, A_0, or activity concentration[a]	Half-life, days	Gamma-ray energies, E_γ, keV	Absolute emission probability,[b] P_γ, per 100 disintegration
Mixed (ampoule)				
^{109}Cd,	11.4 kBq/g	462.6 ± 0.7	88.034	3.65(6)
^{57}Co,	0.41 kBq/g	271.79 ± 0.09	122.061	85.68(3)
^{123m}Te,	0.45 kBq/g	119.7 ± 0.1	159.970	83.99(8)
^{113}Sn,	2.09 kBq/g	115.09 ± 0.04	391.702	64.89(17)
^{137}Cs,	1.87 kBq/g	10999 ± 11	661.660	85.20(3)
^{60}Co	2.11 kBq/g	1925.5 ± 0.5	1173.238	99.89(2)
			1332.502	99.983(1)
			898.042	94.1(5)
^{88}Y	4.26 kBq/g	106.63 ± 0.025	1836.063	99.36(5)
Single ^{152}Eu				
Point	370 ± 5.55 kBq			
Ampoule	472.68 ± 1.75 kBq	4933 ± 11	121.782	24.40(15)
			244.699	7.54(5)
			344.281	26.52(18)
			411.126	2.246(16)
			443.965	3.10(2)
			778.920	12.94(7)
			867.390	4.23(3)
			964.055	14.60(8)
			1085.842	10.09(4)
			1089.767	1.737(8)
			1112.087	13.56(6)
			1212.970	1.423(10)
			1299.152	1.630(10)
			1408.022	20.80(12)
Uranium,	5.907 ± 0.84 kBq			
BL3[c]			241.979	7.12(11)
^{226}Ra[d]			295.207	18.2(3)
			351.925	35.1(4)
			609.318	44.6(5)
			768.364	4.76(7)
			934.060	3.07(4)
			1120.285	14.7(2)
			1238.110	5.78(7)
			1764.515	15.1(3)
			2204.105	4.98(12)

[a] Certified value.
[b] Taken from Ref. 1. Uncertainties are related to the last digits.
[c] Uranium concentration: 1.02±0.01%.
[d] ^{226}Ra in equilibrium with its all daughter products, half-lives from 163 seconds to 22 years.

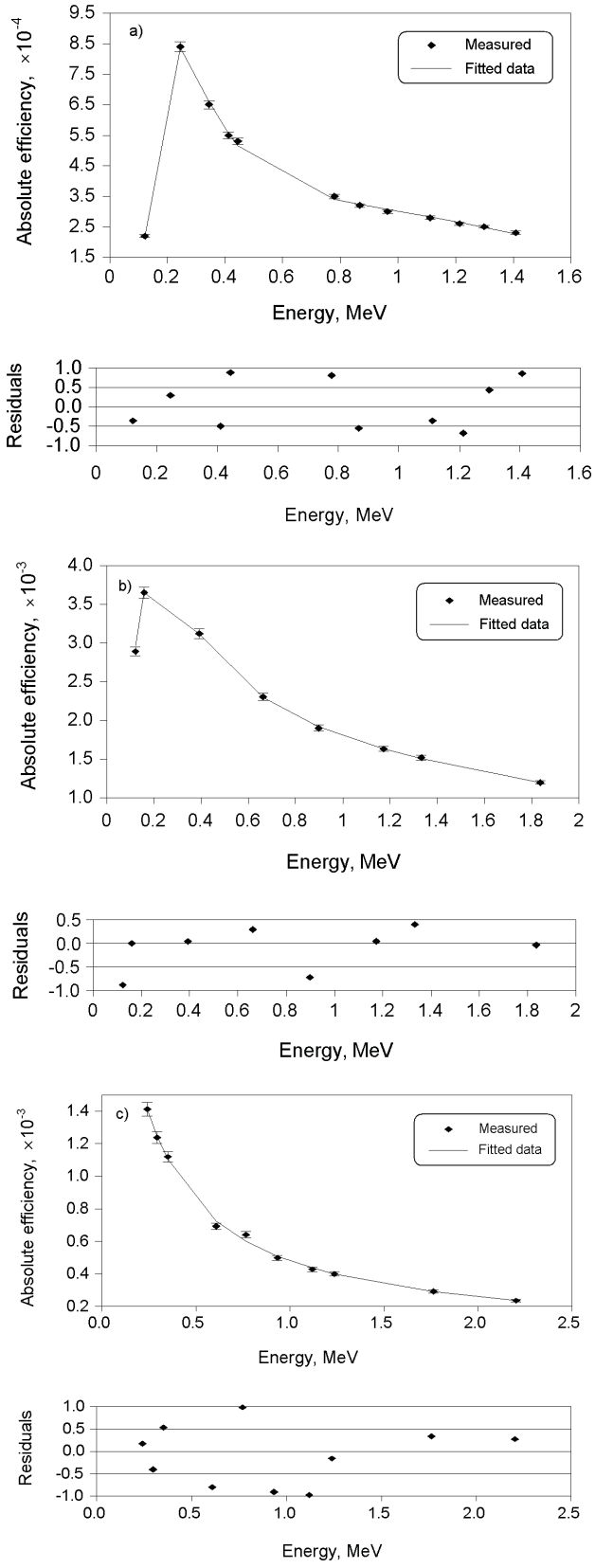

Fig. 2. Efficiency curves of the shielded REGe detector for far irradiation geometry; (a) ^{152}Eu point source (range: 0.1–1.5 MeV; the parameters: $a_0 = 1.0999$, $a_1 = 0.5537$, $a_2 = -0.3937$, $a_3 = -1.0468$, $a_4 = -0.4841$), (b) mixed ampoule (range: 0.1–2.0 MeV; the parameters: $a_0 = -6.3222$, $a_1 = 0.5964$, $a_2 = -0.0313$, $a_3 = -0.0987$, $a_4 = -0.0786$), (c) BL3 uranium standard (range: 0.2–2.5 MeV; the parameters: $a_0 = -0.7344$, $a_1 = -0.8478$, $a_2 = -0.04203$, $a_3 = -0.0206$, $a_4 = -0.0244$)

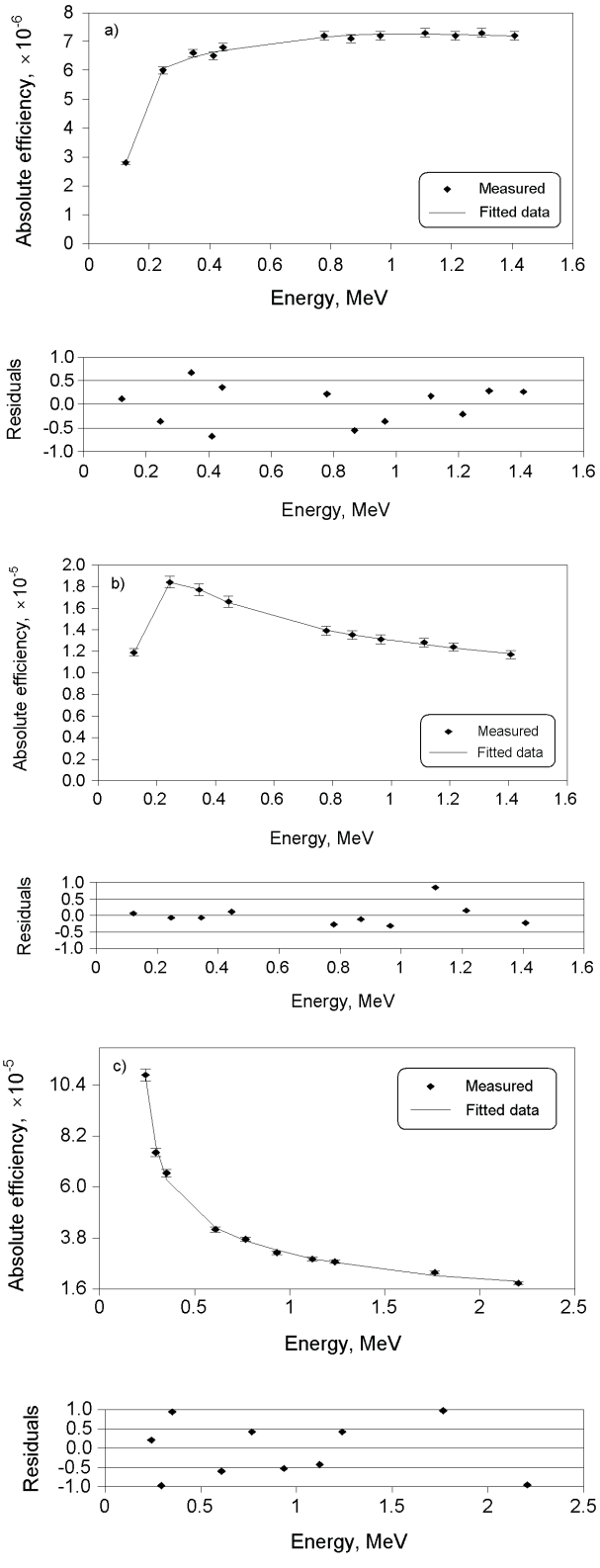

Fig. 3. Efficiency curves of the shielded REGe detector for far counting geometry; (a) ^{152}Eu point source (range: 0.1–1.5 MeV; the parameters: $a_1 = 1.9819$, $a_2 = 2.0026$, $a_3 = 0.8727$, $a_4 = 0.1617$), (b) ^{152}Eu ampoule source (range: 0.1–1.5 MeV; the parameters: $a_0 = 0.2646$, $a_1 = -0.2733$, $a_2 = -0.0129$, $a_3 = -0.1175$, $a_4 = -0.0868$), (c) BL3 uranium standard (range: 0.2–2.5 MeV; the parameters: $a_0 = 1.1462$, $a_1 = -0.6365$, $a_2 = -0.1005$, $a_3 = 0.0425$, $a_4 = 0.1612$)

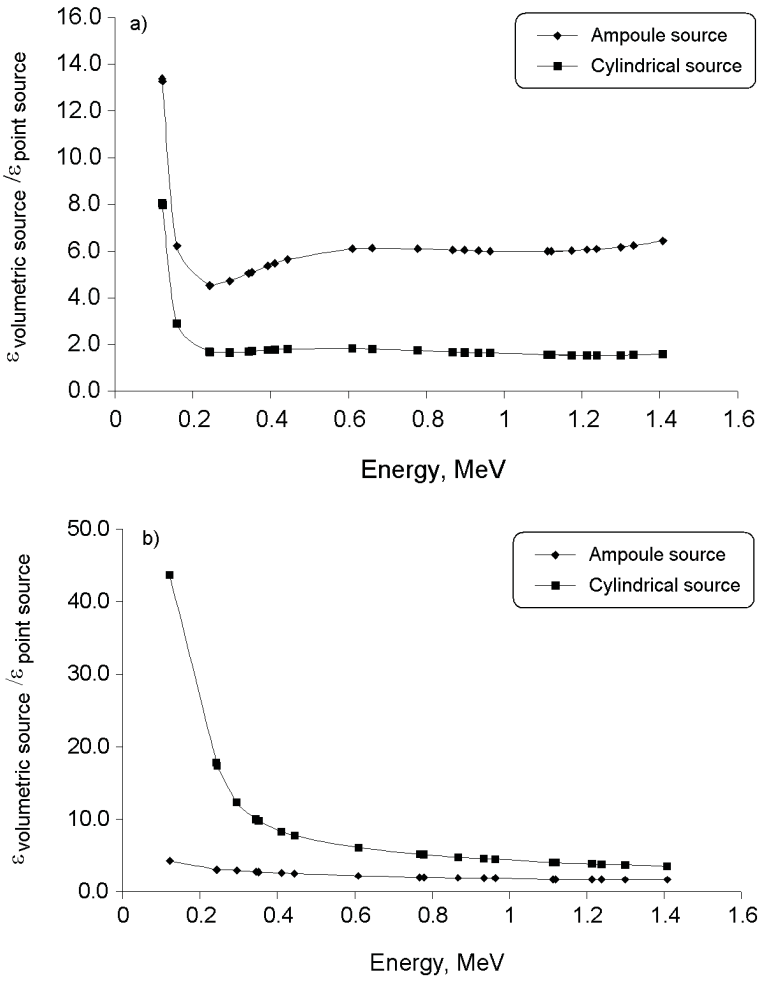

Fig. 4. Efficiency ratios for the voluminous sources; (a) far irradiation geometry, (b) far counting geometry

Discussion

As expected, the FEP efficiencies obtained for the far irradiation geometry are higher than those for the far counting geometry. The shapes of the curves are similar, except for point source at far counting geometry. From Fig. 3a it can be clearly seen that the efficiency curve, obtained for ^{152}Eu point-source geometry differs from the curves of the extended sources, especially from that of the ^{152}Eu ampoule at the same source-to-detector distance (far counting geometry). This may be due to the photon scattering and attenuation for the point source at too far source-to-detector distance because it is different from that for extended source at the same distance.

Conclusions

The absolute FEP efficiencies of REGe detector are measured in the interval of 0.1–2.5 MeV by using different calibration sources (point, ampoule and cylinder) for different source–detector geometries in the presence of Li_2CO_3 powder case and cadmium cover. The efficiency calibrations have not yet completed for higher energy range up to 10 MeV. The measured FEP efficiency data are well fitted to the 4th order polylog functions. In the first configuration, the FEP efficiency is higher than in the second configuration in the order of 10^{-3}–10^{-4}, but the thermal neutron fluence rate at the sample irradiation position is low, in the order of 10^2 n·s^{-1}·cm^{-2}. In the second configuration, the FEP efficiency is lower than in the first configuration, in the order of 10^{-5}–10^{-6} but the thermal neutron fluence rate at the sample irradiation position is 10^4 n·s^{-1}·cm^{-2}. Therefore, the necessary modifications in the source-detector geometry will be made to increase thermal neutron fluence rate and detector efficiency.

*

This study was carried out within the framework of Research Project coded IV.05.DPT.1, supported by Turkish Atomic Energy Authority (TAEA). The author wishes to thank Dr. Haluk YÜCEL and Ahmet DEMIRBAŞ, researchers in SNRTC, for their useful discussion and comments.

References

1. R. N. ACHARYA, K. SUDARSHAN, A. G. C. NAIR, Y. M. SCINDIA, A. GOSWAMI, A. V. R. REDDY, S. B. MANOHAR, J. Radioanal. Nucl. Chem., 250 (2001) 303.
2. M. CRITTIN, J. JOLIE, J. KERN, S. J. MANNANAL, R. SCHARZBACH, J. Alloys Comp., 253–254 (1997) 156.
3. A. G. C. NAIR, K. SUDARSHAN, N. RAJE, A. V. R. REDDY, S. B. MANOHAR, A. GOSWAMI, Nucl. Instr. Meth., A516 (2004) 143.
4. C. YONEZAWA, H. MATSUE, K. MCKAY, P. POVINEC, J. Radioanal. Nucl. Chem., 248 (2001) 719.
5. R. KHELIFI, Z. IDIRI, L. OMARI, M. SEGHIR, Appl. Radiation Isotopes, 51 (1999) 9.
6. ZS. RÉVAY, G. L. MOLNÁR, T. BELGYA, ZS. KASZTOVSZKY, R. B. FIRESTONE, J. Radioanal. Nucl. Chem., 244 (2000) 383.
7. W. AHMAD, M. AHMAD, M. U. RAJPUT, J. Neutron Res., 11 (2003) 145.
8. Ş. TURHAN, H. YÜCEL, A. DEMIRBAŞ, J. Radioanal. Nucl. Chem., 243 (2004) 181.
9. G. L. MOLNÁR, ZS. RÉVAY, T. BELGYA, Nucl. Instr. Meth., A489 (2002) 140.
10. G. L. MOLNÁR, ZS. RÉVAY, R. L. PAUL, R. M. LINDSTROM, J. Radioanal. Nucl. Chem., 234 (1998) 21.
11. R. L. PAUL, R. M. LINDSTROM, J. Radioanal. Nucl. Chem., 234 (2000) 21.
12. K. DEBERTIN, R. G. HELMER, Gamma- and X-ray Spectrometry with Semiconductor Detectors, North-Holland, Amsterdam, 1988, Chapter 4.
13. K. SUDARSHAN, A. G. C. NAIR, R. N. ACHARYA, Y. M. SCINDIA, A. V. R. REDDY, S. B. MANOHAR, A. GOSWAMI, Nucl. Instr. Meth., A457 (2001) 180.
14. S. RAMAN, C. YONEZAWA, H. MATSUE, H. IIMURA, N. SHINOHARA, Nucl. Instr. Meth., A454 (2000) 389.
15. P. H. STELSON, S. R. DICKENS, R. C. TRAMMEL, Nucl. Instr. Meth., 98 (1972) 481.
16. Z. KIS, B. FAZEKAS, J. ÖSTÖR, ZS. RÉVAY, T. BELGYA, G. L. MOLNÁR, L. KOLTAY, Nucl. Instr. Meth., A418 (1998) 374.
17. K. DEBERTIN, Nucl. Instr. Meth., 226 (1984) 566.
18. J. B. WILLETT, Nucl. Instr. Meth., 84 (1970) 157.
19. A. AKSOY, J. Radioanal. Nucl. Chem., 169 (1993) 463.
20. W. R. KANE, M. A. MARISCOTTI, Nucl. Instr. Meth., 56 (1967) 189.
21. P. W. GRAY, A. AHMAD, Nucl. Instr. Meth., A237 (1985) 577.